

# A SURVEY OF GROUND CONDUCTIVITY AND DIELECTRIC CONSTANT IN NORWAY WITHIN THE FREQUENCY RANGE 0.2–10 Mc/s

BY

KARL EMIL ELIASSEN

Norwegian Defence Research Establishment

(Manuscript received 5th October, 1956)

## SUMMARY

Measurements of ground conductivity  $\sigma$  and dielectric constant  $\epsilon$  were carried out at a number of different sites in Southern Norway during the first 8 months of 1955. The wave tilt method was employed for frequencies between 0.2 and 12 Mc/s. The analysis has been based upon K. A. Norton's expression for wave tilt in the radiation field of a vertical electric dipole on a plane, homogeneous earth. As shown by Grosskopf and Wait these effective constants will, for a horizontally stratified ground, depend upon both the specific  $\sigma$  and  $\epsilon$  values of each layer and the ratio of wave length to layer-thickness, the depth of penetration being taken into consideration. Nevertheless these effective ground constants may be applied to every kind of ground wave calculations within a limited frequency range.

Wet bogs and clays in formerly submarine areas show very high effective conductivity,  $\sigma > 10^{-2}$  mho/m. On the contrary granites and gneisses, which are very common in Norway, as well as sand and gravel in glacier and river deposits, are all very poor conductors. Values of  $\sigma$  below  $10^{-2}$  mho/m were frequently observed. Effective dielectric constants are ordinarily between 30 and 50 for the first group, but around 10 for the last. Negative values of  $\epsilon_{eff}$  are common in areas with a surface layer of sand upon clay of much higher conductivity.

Some special investigations were performed in order to study the effect of ice upon fresh water, seasonal variations of effective  $\sigma$  and  $\epsilon$  in a clay area at Kjeller, and the possibility of directional attenuation over an anisotropic ground at Bamble.

## 1.0 INTRODUCTION

It is well known that a certain knowledge of the electrical properties of the ground is required for almost any kind of calculations concerning propagation of radio waves. The complex ground conductivity influences the radiation pattern of aerials intended for communication via the ionosphere or troposphere as well as along the earth's surface. Regarding the latter, the waves will even suffer attenuation and phase change along the entire path due to the presence of a finite conducting ground. Of major importance then is the first part of the path from the transmitter, as stated

by the Millington «land — sea» effect. Consequently ground wave transmitters are ordinarily erected within districts of good conducting ground.

Investigations of ground conductivity at radio frequencies have been carried out in most parts of the world during the last thirty years, but up to 1954 very few measurements had been performed in Norway. However, a geological survey map with a kind of radiogeological classification was made during the last war [31], though no values of ground conductivity, nor dielectric constants were presented.

At the end of 1954 the NDRE made a study of the existing methods by which ground constants could be determined, and comparative measurements were made at Kjeller and Gardermoen [27]. The conclusion was reached that the wave tilt method was the best suited for measurements in Norwegian terrain, and a simple measuring equipment was arranged.

Based on the study of geological maps and reports from measurements abroad a programme was set up to investigate further the conductivity of Norwegian rocks and soil. It was soon recognized, however, that to present a detailed map of measurements covering the whole of Norway would be beyond the limits of economics and practicability. Thus an attempt was made to correct the above mentioned survey map only, and as far as possible add to it values of measured ground constants. According to this programme

measurements were made within a number of selected, different areas of fairly uniform ground. The result is presented here.

It was shown by the measurements that a homogeneous ground, for which the classical Sommerfeld propagation theory was developed, is in fact very rare. Rocks may exhibit a pronounced primary stratification, or, more commonly, may show a surface layer of better conductivity due to a higher moisture content. Within districts of Quaternary deposits a three layer ground is common, the mid-layer being the best conducting. In addition seasonal and diurnal variations in temperature and moisture content occur, changing the state of stratification markedly.

Owing to this the theory of horizontal stratification was paid some attention, and a few special cases were treated more thoroughly.

## 2.0 PROPAGATION OF SURFACE WAVES ALONG A FINITELY CONDUCTING PLANE EARTH

The exact solution of Maxwell's equations in the case of radio waves radiated along the surface of earth from a vertical electric doublet or a short vertical aerial on the earth, may be carried out for certain cases. A most complicated mathematics is involved, however, and it is of utmost importance for practical applications to introduce general simplifications.

Though it is far beyond the scope of this paper to give any new propagation theory, an attempt is made to present basic formulae on a form convenient for an analysis of field measurements. Further an evaluation of the field equations for a plane wave propagating over a stratified earth is carried out to explain some discrepancies between the theory of homogeneous earth and measurements carried out on a stratified ground. This problem was first treated by Hack in 1903 and later by Grosskopf [3-5] and Wait [8-10].

### 2.1 Effective ground constants.

The surface wave field intensity at a short distance,  $d$ , from a vertical electric dipole, is, according

to the classical Sommerfeld-Norton theory given by the following formula:

$$E = E_0 \frac{F}{d} (\mathbf{k} + \mathbf{r} \sqrt{n^2 - 1} / n^2) \quad (2.01)$$

By short distance is meant that we can neglect the curvature of earth.  $E_0$  is the free-space field intensity at a unit distance from the aerial,  $\mathbf{k}$  and  $\mathbf{r}$  are unit vectors in the vertical direction and in the direction of propagation respectively. The attenuation function  $F$ , shown in equation (2.07), as well as the refractive index  $n$ , depend upon the frequency  $\omega$ , the ground conductivity  $\sigma$  and the dielectric constant  $\epsilon$ . The time factor  $e^{i\omega t}$  is neglected.

$$n = \sqrt{\epsilon_r - j\bar{X}} \quad (2.02)$$

$$X = \sigma / \omega \epsilon_0 \quad (2.03)$$

In the mks-system of units, the dielectric constant  $\epsilon$  is measured in F/m and written as the product of the dielectric constant of free space  $\epsilon_0 = 8,854$  F/m and the relative dielectric constant  $\epsilon_r$ . The

latter characterizes the electric properties of the soil together with the conductivity  $\sigma$ , which is measured in mho/m. These two are mentioned the ground constants. The relative magnetic permeability is neglected, since it usually equals unity.

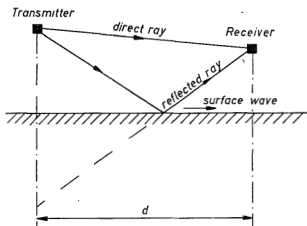


Fig. 2.1 The ground wave components.

Equation (2.02) is valid for a homogeneous earth only. With stratification the refractive index will change relative to the layer thickness and the electric properties of each layer.

When the frequency is kept constant, radio measurements ordinarily give two independent magnitudes, and a complete investigation of a stratified ground requires measurements at different frequencies. As far as  $\epsilon$  and  $\sigma$  in each layer do not change with the frequency, these constants may be determined together with the depth of each layer.

The ratio between the horizontal and the vertical components of the electrical field is easily derived from (2.01):

$$E_r/E_z = \rho e^{i\varphi} = \sqrt{n^2 - 1}/n^2 \quad (2.04)$$

This ratio is called the wave tilt, and the expression is of fundamental importance in the ground wave propagation theory. The «numerical distance»  $\phi$  introduced by Sommerfeld may for instance be expressed as:

$$\phi e^{i\theta} = -j(kd/2)[\rho e^{i\varphi}]^2 \quad (2.05)$$

Here  $k$  is the phase constant  $2\pi/\lambda$ , where  $\lambda$  denotes wave length. Hence we may write phase and magnitude separately:

$$b = 2\varphi - \pi/2$$

$$\phi = \pi d \rho^2 / \lambda$$

From  $\phi$  and  $b$  the attenuation function  $F$  is expressed, according to Sommerfeld, as

$$F = 1 + j\sqrt{\phi} e^{-\phi} 2 \int_0^{\infty} \frac{e^{-u^2}}{-j\sqrt{\phi}} du \quad (2.06)$$

The function  $F$  is presented in Fig. (2.2). Some authors use the opposite sign for  $b$  in the equation above, because  $e^{-j\omega t}$  is chosen as time factor, for instance K. A. Norton for his field strength curves [7].

Further the reflection coefficients for plane waves may be expressed directly from  $\rho$ ,  $\varphi$  or as functions of  $\phi$ ,  $b$  [7].

Grosskopf [5] and Wait [9, 10] have shown that the different propagation formulae exist in the same form even for a horizontally stratified ground. This fact enables us to solve a wide variety of practical problems concerning ground wave propagation if the terms  $\rho$  and  $\varphi$  only, or any two terms derived directly from these, are known. But it is obvious that a further simplification by introducing an «effective conductivity» as the only

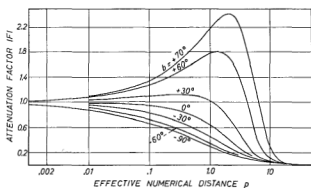


Fig. 2.2. The attenuation function  $F$  versus numerical distance  $\phi$  (after Wait),  $b < 0$  for a homogenous earth.

significant ground constant, can not be generally accepted.

For most radio measurements, however, the result is not presented as  $\rho$  and  $\varphi$  values, but in terms of effective ground constants  $\epsilon_{eff}$  and  $\sigma_{eff}$  which are determined from the propagation formulae as if the earth were homogenous, i.e. related to  $\rho$ ,  $\varphi$  by equation (2.02—4), shown in Fig. (2.3).

For a homogenous ground  $\epsilon$  and  $\rho$  will be fairly invariable for increasing frequency above 100 kc/s; see also chapters 4 and 6. For a stratified

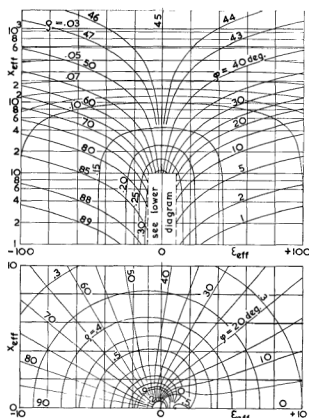


Fig. 2.3. The wave tilt  $q^e/\varphi$  as a function of effective ground constants  $\epsilon_{\text{eff}}$  and  $X_{\text{eff}}$ .

ground, on the other hand, the effective constants are valid only within a limited frequency range. They are not true material constants, and in some cases their value have no physical meaning, as, for instance, the effective dielectric constant may be negative.

## 2.2 Stratification in the earth's surface.

The different propagation formulae, including the Sommerfeld attenuation function, are all so close related to the wave tilt that only the latter will be treated here. The wave tilt will be derived for a plane wave travelling along a horizontally stratified earth and the result compared with equation (2.04). The evaluation is based upon Grosskopf's and Wait's papers. It will be shown later that for most practical applications the result is valid even for the radiation field from a vertical aerial.

Maxwell's equations give us the field components of a plane wave travelling in the  $x$ -direction in a medium  $m$ , illustrated in Fig. (2.4), as:

$$H_{my} = (a_m e^{-u_m z} + b_m e^{u_m z}) e^{-j k x}$$

$$E_{mx} = -\frac{1}{\sigma_n + j\omega \epsilon_m} \frac{\partial H_{my}}{\partial z} \quad (2.07)$$

$$E_{mz} = \frac{-1}{\sigma_m + j\omega \epsilon_m} \frac{\partial H_{my}}{\partial z}$$

$a_m$  and  $b_m$  are arbitrary constants. The propagation constants,  $u$  in the  $z$ -direction, and  $j h$  in the  $x$ -direction, must be related to the complex propagation constant  $\gamma$  of the medium by:

$$u^2 = h^2 + \gamma^2_m$$

$$\gamma^2_m = j\sigma_m \mu_m \omega - \epsilon_m \mu_m \omega^2 \quad (2.08)$$

The magnetic permeability  $\mu$  is in most rocks and soil equal to the permeability of free space,  $\mu_0 = 4\pi \cdot 10^{-7} \text{ H/m}$ .

By solving (2.07) for  $m = 0$  and  $a_0 = 0$ , we find the general expression for the wave tilt:

$$q^e/\varphi = E_{ox}/E_{oz} = -j u_0/h \quad (2.09)$$

and the propagation constant  $h$  will be found from the boundary conditions in each case by eliminating  $a$  and  $b$  from equation (2.07).

For a homogenous earth, there is only one boundary between different media, namely between the air (0) and ground (1), and  $h$  is explicitly derived from:

$$h = \omega \sqrt{\epsilon_0 \mu_0} \sqrt{(1 - \mu/\mu_0 \epsilon')/(1 - 1/\epsilon'^2)} \quad (2.10)$$

The complex dielectric constant  $\epsilon'$  replaces  $\epsilon_j - jX$  for the sake of simplicity.

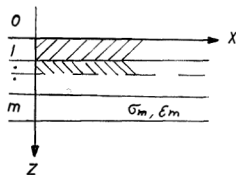


Fig. 2.4. Geometry of a stratified earth.

When  $\mu = \mu_0$  (2.09) gives:

$$q^e/\varphi = E_{ox}/E_{oz} = 1/\sqrt{\epsilon'} = 1/n \quad (2.11)$$

It is clear that  $q^e$  will be less than unity, and  $\varphi$  will never exceed  $45^\circ$ .

For all  $n^2 \gg 1$  it is further seen that equation (2.04) gives the same result as equation (2.11), a fact which indicates that Sommerfeld's surface wave is related to the Zenneck-wave.

A common sort of inhomogeneity is the horizontal stratification in two layers, one upper layer (1) with the depth  $Z$ , and a second (2) whose depth may be considered infinitely large. From equation (2.07) we obtain 9 equations. The three propagation constants are mutually related by:

$$\begin{aligned} \gamma_o^2 &= -\omega^2 \epsilon_o \mu_o \\ \gamma_{1,2}^2 &= \gamma_o^2 \epsilon'_{1,2} \text{ for } \mu_{1,2} = \mu_o \end{aligned} \quad (2.08b)$$

Since the field in no case can be allowed to approach infinity for increasing  $z$ , we always have  $a_o = b_o = 0$ . The remaining  $a$ 's and  $b$ 's are eliminated by introducing the boundary conditions in equation (2.07) from which we obtain a transcendental system of equations for determining  $h$ :

$$h^2 = \gamma_o^2 [1 - Q^2 / \epsilon'_1] / [(Q / \epsilon'_1)^2 - 1] \quad (2.12)$$

$$\begin{aligned} Q &= -\left(\frac{\gamma_1}{\gamma_o}\right)^2 \frac{u_o}{u_1} = \frac{\delta \sinh u_1 Z + \cosh u_1 Z}{\delta \cosh u_1 Z + \sinh u_1 Z} \\ \delta &= \left(\frac{\gamma_2}{\gamma_1}\right)^2 \frac{u_1}{u_2} = \frac{\epsilon'_1 \epsilon'_2}{\epsilon'_2 \epsilon'_1} \end{aligned} \quad (2.13)$$

The dimensionless ratios  $Q$  and  $\delta$  are ratios of wave impedance in the different media. Now the wave tilt may be expressed by (2.09) and (2.12) as

$$\rho' e^{i\varphi'} = \sqrt{1/\epsilon'_1} \sqrt{(\epsilon'_1 - 1) / (\epsilon'_1 / Q^2 - 1)} \quad (2.14)$$

By the first sight this last expression does not tell us any more than equation (2.09), as far as  $Q$  is not known. After some simplifications, however, it turns out to be a very useful expression. For  $\epsilon'_1 \gg 1$ , which is valid in a number of practical cases,  $h^2 \approx -\gamma_o^2$ , for all practical values of  $Q$ . Then

$$\begin{aligned} \delta &\approx \sqrt{(\gamma_1^2 - \gamma_o^2) / (\gamma_2^2 - \gamma_o^2)} (\gamma_2 / \gamma_1)^2 \\ &= \frac{\sqrt{\epsilon'_1 - 1}}{\epsilon'_1} \frac{\epsilon'_2}{\sqrt{\epsilon'_2 - 1}} \end{aligned} \quad (2.15)$$

and the wave tilt

$$\rho' e^{i\varphi'} \approx Q \rho_1 e^{i\varphi_1} \quad (2.16)$$

The last expression states that the wave tilt over a two layer ground may be derived directly from the expression for a homogeneous earth by applying

a correction factor  $Q$ , which in virtue of the relation between the different hyperbolic functions may be written

$$Q = \tanh(\alpha + u_1 Z) \quad (2.17)$$

provided that  $\tanh \alpha = 1/\delta$ .

Curves of  $Q$  which show magnitude and phase for different functions of  $\delta$  are published by Grosskopf [2] and Wait [8]. One example is shown in Fig. (2.5). These curves give values of  $Q$  to be applied to the low frequency range where  $\epsilon$  is of secondary importance compared with  $\sigma$ . For a more general solution of (2.17) a «tanh-relief» [11] or a modified Smith chart may be used.

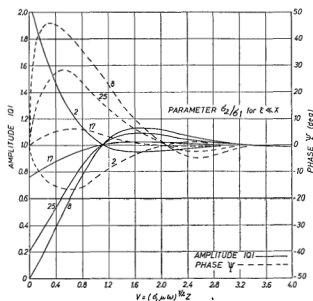


Fig. 2.5. The correction factor  $Q$  versus numerical depth  $V = \sqrt{\sigma \mu \omega} Z$  for different ratios  $\sigma_2/\sigma_1$ , (after Wait).

In some cases equation (2.16) is inconvenient. For instance when expected seasonal variations in the effective ground constants are to be calculated from measured values under «normal» conditions, it will be necessary to evaluate the wave tilt by a correction of the  $\rho$ 's and  $\varphi$ 's primarily based upon the constants of the lower medium. It is supposed then that  $\epsilon_2$  and  $\sigma_2$  are the known quantities, and  $\rho'$ ,  $\varphi'$  should be calculated when an upper layer (1) caused by frost or drought etc. is built up in the surface.

A simple modification of (2.13) gives

$$M = \delta Q = -\epsilon'_2 u_o / u_2 = \delta \tanh(\alpha + u_1 Z) \quad (2.18)$$

and  $h$  is obtained from an expression similar to (2.12):

$$h^2 = \gamma_0^2 [1 - M^2 / \epsilon'_2] / [(M / \epsilon'_2)^2 - 1] \quad (2.19)$$

hence

$$\rho' e^{i\varphi'} = \sqrt{[(\epsilon'_2 - 1) / \epsilon'_2] / [(\epsilon'_2 / M^2 - 1)]} \quad (2.20)$$

Even if a poor conducting upper layer prevents  $\epsilon'_1$  from being large compared with unity, a moderate depth  $Z \ll \lambda$ , and moderate or good conductivity in the subground give  $\epsilon'_2 \gg M^2$  which enables us to simplify even this expression to

$$\rho' e^{i\varphi'} \approx M \rho_2 e^{i\varphi_2} \quad (2.21)$$

and the simplified expression for  $\delta$  in equation (2.15) is still valid.

From the expressions for the correction factor  $Q$  and when Fig. (2.2) is compared with Fig. (2.5) we conclude:

- In the low frequency range a poor conducting upper layer causes  $\varphi'$  to be large and it may even exceed  $45^\circ$ . For values of  $\varphi'$  greater than  $45^\circ$ ,  $\epsilon_{eff}$  will be negative, and one measurement alone will be the proof of existing stratification.  $\rho'$  increases from  $\rho_2$  towards  $\rho_1$  by increasing layer thickness  $Z$ , and it may even be greater than  $\rho_1$ .
- On the contrary, a good conducting upper layer causes  $\varphi'$  to be small, and large  $\epsilon_{eff}$  values will be derived.
- For higher frequencies where  $\epsilon$  is of greater importance,  $\varphi_{1,2}$  is ordinarily small, but stratification with  $\epsilon'_1 < \epsilon'_2$  may give considerable  $\varphi'$  values, and large values of  $\epsilon_{eff}$  will be the result. This may easily mislead to the conclusion that the conductivity of each layer increases with increasing frequency.

As a result of point c) a warning must be given against studies of the frequency dependence of the real ground constants based upon wave measurements. Only by isolating a limited amount of soil in a laboratory test condenser it will be possible to avoid the influence of stratification.

The general solution of the stratification problem for a large number of horizontal layers has been found by Wait. The expression is derived in just the same manner as for the two layer case, from equation (2.07). Unfortunately it has not been possible to give the equations a form plain enough for practical calculations. Graphical superposition

from the two-layer model seems to be the most useful way of solving more complicated problems.

Equation (2.14) and (2.20) are valid for plane waves over a two-layer ground, and it is easily seen by comparison with equation (2.11) that we have found an expression for the refractive index  $n'$  for a stratified ground. The same result could be derived by starting with the laws of reflection. As a principle,  $\rho'$  and  $\varphi'$  could even be expressed from equation (2.04) for a stratified ground. We saw, however, that when the expressions in question were simplified to a form which may find practical application, we had to require  $n_2^2 \gg 1$  in (2.14—16) or  $n_2^2 \gg 1$  in (2.20—2.21), and that is just the same condition which makes the expressions derived for plane waves valid even for waves radiated from an aerial at some distance.

The restriction  $n^2 \gg 1$  is not severe since for most rocks and soil  $X$  alone is far greater than unity through the entire LF and MF band, and for good conducting soil far into the VHF band. For some types of soil  $\epsilon_r$  is large enough to make  $n^2 \gg 1$  for all frequencies. The same expressions may therefore be applied to practical field measurements without further modifications.

### 2.3 Depth of penetration.

In the last chapter the problem of stratification in the earth surface was mentioned without paying any attention to the actual depth which must be taken into consideration. The depth of penetration may be calculated in the same manner as the «skin depth» of currents in a plane conductor. Fig. (2.6) shows some curves which illustrate this. The limit of penetration is in Fig. (2.6) chosen as the depth where the electric field is reduced to  $1/100$  of the field at the surface. The curves give a general view, nothing is told, however, about the thickness required for an upper layer to act as infinitely deep in practical measurements.

The «effective depth of penetration» may be evaluated from equation (2.17) where the correction factor  $Q$  is given as a function of the thickness  $Z$  of an upper layer:

(2.22)

$$|Q| e^{i\varphi} = \tanh(\alpha + \alpha_1 Z) = \tanh(\alpha + Z \sqrt{\gamma_1^2 + h^2})$$

where  $\gamma_1$  is a frequency dependent function of the ground constants in the surface layer,  $h$  is to a

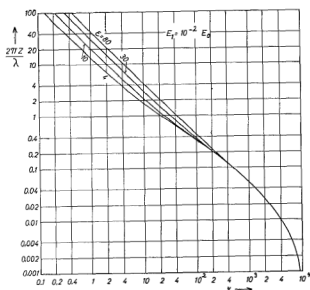


Fig. 2.6. Depth of penetration by grazing incidence of vertically polarized radio waves, (after Pfister).

large extent determined by  $\gamma_0$  alone and  $a$  by the ratio between ground constants in the surface layer and the sub-soil.

If then, at a given frequency,  $|Q - 1|$  and  $|\psi|$  for all possible  $a$  never exceed the priorly chosen small values  $\Delta Q$  and  $\Delta\psi$  respectively, for increasing  $Z > Z_0$ , we may regard  $Z_e$  as the effective depth of penetration.

The limits  $\Delta Q$  and  $\Delta\psi$  should be chosen in accordance with the accuracy obtainable by the actual measuring equipment.

Provided that  $\gamma_1^2 \gg \gamma_0^2$ , we may write

$$|Q|e^{i\psi} = \tanh(\alpha + Z \sqrt{\omega^2 \mu_0 \epsilon_0 (-\epsilon'_1)}) \quad (2.23)$$

and from a tanh-relief the limits are found in each case. Even the last expression may be simplified to some extent. For instance for  $X \gg \epsilon_1$ ,  $(-\epsilon'_1)$  may be replaced by  $jX$ , and

$$\begin{aligned} |Q|e^{i\psi} &= \tanh(\alpha + u_1 Z) \\ &= \tanh(\alpha + Z \sqrt{\omega \mu \sigma / 2} + jZ \sqrt{\omega \mu \sigma / 2}) \quad (2.24) \end{aligned}$$

In agreement with Fig. (2.5) we find  $|\psi| < 3^\circ$  and  $|Q - 1| < 2\%$  for all  $Z \sqrt{\omega \mu \sigma} > 3$ , thus no measurable change in the field will be introduced by the presence of a discontinuity deeper than

$$Z_e = \frac{3}{\sqrt{\omega \mu \sigma}} \quad (2.25)$$

This last expression states that for large  $X$ ,  $Z_e$  is inversely proportional to the root of the frequency. When the frequency  $f$  is measured in Mc/s and the conductivity in mmho/m, we obtain

$$Z_e \approx \frac{34}{\sqrt{\sigma f}} \quad (2.25b)$$

This means about 2–3 m for good conducting soil at 10 Mc/s and up to 10 times as much for poor conducting soil up to this frequency or for a good conductivity around 100 kc/s.

Because of the periodical nature of  $\tanh(a + jb)$  the last expression will not hold for values of  $\epsilon_1$  of the same order of magnitude as  $X$ . This will be clearly demonstrated by regarding equation (2.17) for  $\epsilon \gg X$ , i.e. for  $\omega \epsilon \gg \sigma$ :

$$Q = \tanh(\alpha + u_1 Z) = \tanh(\alpha + j\omega Z \sqrt{\mu_0 \epsilon_0 \epsilon_1}) \quad (2.26)$$

In this case only the imaginary term of the argument is increasing with  $Z$ , and no limit  $Z_e$  will be found. In other words, we have wave propagation in a lossless dielectric medium, and any inhomogeneity will be able to influence the surface wave by introducing reflections.

No conclusion will be drawn about the applicability of this fact to different geophysical investigations. It may be of practical importance, but in most cases it seems to be difficult to fulfill the requirement  $\epsilon_1 \gg X$ . Neither must it be forgotten that the evaluation of (2.25) is based upon plane waves. For radiogeological mapping, however, it is advantageous to have a great depth of penetration since this will reduce the influence of seasonal and diurnal variations of conductivity in the upper surface layers, caused by changing temperature and humidity.

### 3.0 THE WAVE TILT METHOD APPLIED FOR DETERMINATION OF EFFECTIVE GROUND CONSTANTS

A number of different methods for determining ground constants have been presented during the last thirty years. They are mainly divided into two different groups, namely those which are related to ground wave propagation and those which are not. The last group includes all laboratory sample tests by means of condensers or electrodes on cylinders of rock, as well as measurements of voltage and current between submerged electrodes. Closely related to this group are also measurements on Lecher wires in the earth and measurements of inductance on wires along the earth.

The first group consists of four different systems:

- a) Field strength attenuation measurements,
- b) The wave tilt method,
- c) Determination of reflection coefficients by oblique or vertical incidence,
- d) Height gain registrations.

These four all have the advantage that they give average values for a certain area in terms of effective ground constants. When other methods are applied, these average values are not derived without complicated calculations based upon a large number of measurements within the area and to different depths. It seems reasonable therefore that one of the four methods a—d) should be employed for mapping, but they are not equally simple to execute. The first requires a fairly uniform ground in a straight path extended several wave-lengths from the transmitter, a plane earth, transportable high precision field strength measuring equipment and a transmitter stable enough to give a constant output over a large interval of time.

The last two methods both require some means of elevating the measuring equipment to heights comparable with the wave length. The electrical precision must also be fairly high, except for some reflection measurements developed by Feldman [15].

The wave tilt-method also requires a uniform earth and a plane ground, but only within a small

area around the measuring equipment. No elevation of the equipment is necessary, and a complete measurement is performed in a few seconds. Theoretically there is no doubt therefore, that the wave-tilt method is best suited for mapping in Norwegian terrain. This assumption was further verified by a number of comparative measurements at NDRE during 1954 [27].

The wave-tilt method involves a determination of the state of polarisation in the surface wave from a vertical transmitting aerial on the earth. At a large distance from the transmitter the surface wave is elliptically polarised according to equation (2.02). The form and inclination of the polarisation ellipse are determined by  $\epsilon_{eff}$ ,  $\sigma_{eff}$  and the wave length only. The distance should be at least  $3-4 \lambda$ .

#### 3.1 Technical informations concerning the measuring equipment and the measuring procedure.

A rotating rod aerial 2.5 m long of 1 cm aluminum tubing was positioned about 2 m above the ground as shown by Fig. (3.1). The vertical position was determined by means of a spirit-level. From the center of the aerial a screened twin cable went horizontally through a bakelite tube for the

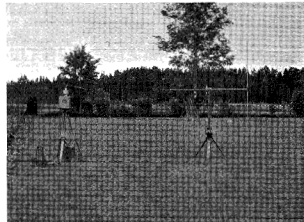


Fig. 3.1. The measuring equipment 1954.



first 2 m and then straight backwards 3 m to the receiver. The cable was connected to an antenna coil, electrostatically screened and inductively coupled to the balanced, tuned input circuit of the receiver. For most of the measurements a copper box with interchangeable plug-in coils was employed, but for the last measurements improved coils were made with individual boxes of silver-plated brass, one for each frequency range, as shown in Fig. (3.3). A special double-screened impedance transformer with ferrite core was developed for better matching between the aerial and the cable, but unfortunately these experiments were not finished until the mapping to be described here was brought to an end. The purpose of these improvements was to obtain a higher accuracy, especially for the investigation of stratified ground.

The receivers were of the Rhode & Schwarz type HHF BN 1500—1501. The entire equipment could be packed and carried by two persons.

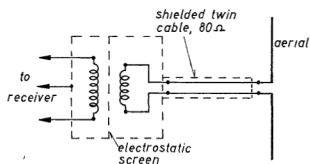


Fig. 3.2. Schematic diagram of input circuit.

Within the district to be examined, some plane sites had to be found. A stabilized transmitter with approximately 100 W input, with a 10 m vertical aerial was erected in the vicinity. The direction of wave propagation on the measuring site was determined by means of a loop aerial on the receiver. Next the rotating rod apparatus was situated so the aerial could be rotated in the plane of incidence of the arriving waves. The loop was then replaced by the screened input coils and the receiver calibrated by means of an internal calibration oscillator.

The tilt angle,  $\theta$ , the ratio between minimum and maximum induced voltage,  $K$ , as well as the ratio between the horizontal and the vertical field component,  $\sigma$ , were determined by direct readings on the logarithmic scale of the instrument and the angular scale on the aerial when the rod was rota-

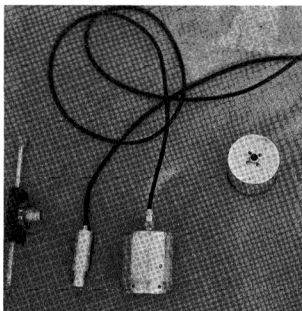


Fig. 3.3. Two new screened coils together with an aerial holder and an experimental ferrite-transformer.

ted. The induced voltage in the aerial as a function of rotating angle is shown in Fig. (3.4).

All measurements were repeated 3—4 times to reduce observation errors.

### 3.2 Analysis of wave tilt measurements.

When  $K$  and  $\theta$  are measured,  $\epsilon_{eff}$  and  $X_{eff}$  will be derived from the nomograph Fig. (3.5 D), and  $\sigma_{eff}$  then from Fig. (3.5 C) or equation (2.03).

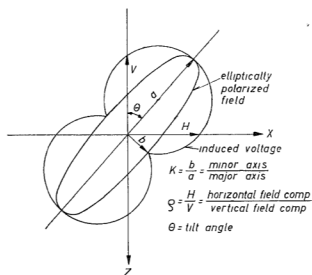


Fig. 3.4. Typical pattern of induced voltage in a short electrical dipole rotated in the plane of incidence.

The axial ratio and the tilt-angle of the polarization ellipse are found by introducing the time factor  $e^{i\omega t}$  in equation (2.04) and then taking the real part of the expression for the vertical and the horizontal components separately:

$$z = \cos \omega t$$

$$x = \rho \cos(\omega t + \varphi) \quad (3.01)$$

By rotation of the coordinate system and elimination of  $\omega t$  we obtain

$$\tan 2\theta = \frac{2\rho \cos \varphi}{1 - \rho^2} \quad (3.02)$$

$$K = \sqrt{\frac{\rho^2 + \tan^2 \theta - 2\rho \cos \varphi \tan \theta}{1 + \rho^2 \tan^2 \theta + 2\rho \cos \varphi \tan \theta}} \quad (3.03)$$

or in the opposite order

$$\rho = \sqrt{\frac{K^2 + \tan^2 \theta}{1 + K^2 \tan^2 \theta}} \quad (3.04)$$

$$\varphi = \cos^{-1} \frac{(1 - K^2) \tan \theta}{\sqrt{(1 + K^2 \tan^2 \theta)(K^2 + \tan^2 \theta)}} \quad (3.05)$$

It is obvious then that measurement of  $K$  and  $\theta$  is adequate for determination of  $\varepsilon$  and  $\sigma$ , as far as these may be derived from  $\rho$  and  $\varphi$  by equations (2.02), (2.03) and (2.04).

The equations (3.02–05) may be simplified within different  $X$ -intervals, and Fig. (3.5 D) is plotted by computing  $K$  and  $\theta$  for different  $\varepsilon$  and  $X$ .

As mentioned before even  $\rho$  is measured, and since only  $K$  and  $\theta$  are used to determine  $\varepsilon$  and  $X$ ,  $\rho$  may be used to check the values derived. If the measurements are correctly performed,  $\rho$ ,  $\theta$  and  $K$  must suit equation (3.04).

Equation (3.02) may be employed to derive  $\varphi$  from  $\theta$  and  $\rho$ , and the equation is shown in a nomographic representation in Fig. (3.5 A). It was found by the measurements, however, that for most cases the  $X$ -values were so large that the simple expression:

$$K = \rho \sin \varphi \quad (3.06)$$

could replace equation (3.03). At the same time small tilt angles occur.  $\varphi$  was then calculated from equation (3.06) and the check carried out by calculation of  $\theta'$  from

$$\tan \theta' = \rho \cos \varphi, \quad (3.07)$$

this angle was compared with the tilt angle mea-

sured. The equations (3.06–07) are shown in a nomograph Fig. (3.5 B).

In the most typical cases of stratification Fig. (3.5 D) could not be used in its original form. For large  $X$ -values, i.e. for small tilt angles, the effective conductivity was derived from

$$X \approx \frac{1}{2} (1/K)^2. \quad (3.08)$$

This gives a practical means for comparison between different sites. The dielectric constant is neglected, but the  $X$  value yields sufficient information for the calculation of ground wave attenuation etc. by low frequencies, without introducing  $\varepsilon$  [6].

For more accurate studies  $\rho'$  and  $\varphi'$  were applied to the theory outlined in chapter 2.2.

### 3.3 Accuracy of the wave tilt measurements.

The equipment employed was too rough to allow high precision measurements, though the degree of accuracy was found to be good compared with ordinary field strength measurements. The different sources of error are:

- Instrument errors.
- Observation errors, on voltmeter.
- Transmitter instability.
- Deviation from true vertical at zero angle.
- Errors on angular scale.
- Electrical asymmetry in input circuit.
- Erroneous minimum detection.
- Field disturbances in arriving waves.
- Inaccurate calculations.

The receivers are specified for  $\pm 20\%$  accuracy by field strength measurements, but  $\pm 5\%$  for voltage measurements. By these relative voltage measurements within few seconds of time the accuracy is probably better, but to find the limit values we put maximum error in the ratio  $K$  due to a) equal to

$$\Delta K_a = 10\%$$

In addition b) and c) are involved. By taking the mean value of the readings with the aerial turned  $180^\circ$ , less than  $5\%$  error will occur. This gives

$$\Delta K_{max} \approx 13\%$$

The same procedure of mean readings reduces even e–g, so the total angular error does not

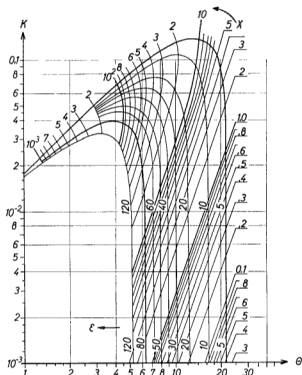
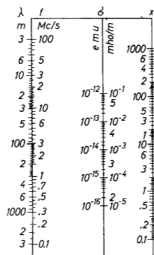
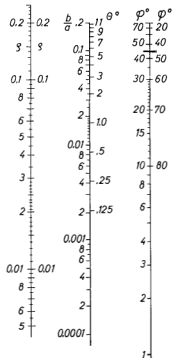
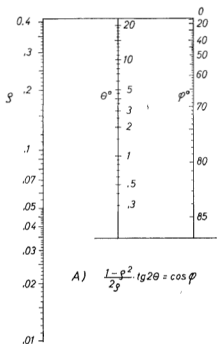


Fig. 3.5. Nomographs for analysis and check of wave tilt measurements.

exceed  $0,8^\circ$  even when the angle of minimum induced voltage could diverge  $1^\circ$  in the two opposite positions owing to f) and g).

The field disturbances caused by uneven ground and large obstructions near the measuring site, cannot be calculated. From measurements just behind large buildings or on steep hills the result is obviously not valid for evaluation of ground constants [27], but by careful selection of plane, open sites for about  $\lambda/2$  to each side in the direction of propagation, no detectable error is introduced.

As the exact formulae for calculation of  $\varepsilon$  and  $\sigma$  are somewhat complicated, nomographs were used, and about 2% error could be introduced by this. By reproducing all measurements 3—4 times and calculating the mean value, the maximum errors are reduced to

$$\Delta K \approx 13/\sqrt{3} \approx 8\%$$

$$\Delta \theta \approx 0.5^\circ$$

The effect of these errors on  $\varepsilon$  and  $\sigma$  is shown in Fig. (3.6).

With regard to studies of stratification,  $\varrho$  will be given with approximately the same limit of error as  $K$ , or somewhat greater because of point d). We may take account for this by adding 2%, and obtain by three measurements

$$\Delta \varrho' \approx \frac{13+2}{3} = 9\%$$

When  $\varphi'$  is calculated from  $K$  and  $\varrho'$ , the errors depend upon the magnitude of  $K/\varrho'$ , and  $\Delta \varphi'$  is approximately 17% for small values of  $K/\varrho'$ . For large ratios the error will be too great to give any reliable value of  $\varphi$ , and equation (3.02), shown in Fig. (3.5 A), will give much higher accuracy, at least for tilt-angles greater than  $2^\circ$ .

The measuring equipment in its original form will not give reliable values of  $\varphi$  for  $\theta < 2^\circ$ . This is the main reason why the improvements mentioned in chapter 3.1 were introduced for further stratification studies.

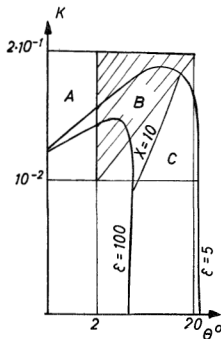


Fig. 3.6. Limits of resulting error by the wave tilt measurements.

- A)  $\theta < 2^\circ$ ,  $K$  cannot be evaluated, but is of minor importance,  $\sigma$  is derived from equation (3.08),  $\Delta \sigma_{\max} = 16\%$ .  
 B)  $\theta > 2^\circ$ ,  $K$  large. No simplified formula exists. The nomograph gives a rough approximation of  $\varepsilon$  for small  $\theta$ , and up to 10% accuracy by increasing  $\theta$ .  $\sigma$  is to a large extent determined by  $\theta$ , the accuracy increases from 25 to 10% by increasing  $\theta$ .  
 C)  $\theta > 2^\circ$ ,  $K$  small.  $\varepsilon$  is determined by  $\theta$  only, with about 10% accuracy.  $\sigma$  depends upon both  $K$  and  $\theta$ , maximum error increases from about 10% by large  $\theta$  and  $K$ , up to 50% by small values of  $\theta$  and  $K$ .

#### 4.0 A SHORT REVIEW OF MEASUREMENTS IN OTHER COUNTRIES

The influence of a finitely conducting ground upon radio waves was explained in detail more than 50 years ago by Hack, Zenneck and Sommerfeld, but very little was published about the actual values of the ground constants at radio frequencies until 1925 [12]. After that time, however, a large number of measurements have been carried out

all over the world. Most of the reports from these measurements describe different measuring methods and present values of  $\varepsilon$  and  $\sigma$  for certain areas [13, 15, 16, 19, 21, 22, 23, 25, 26].

The purpose of these radio-geological explorations has not only been to give basic information for constructors of radio stations, but also to find

new methods for geophysical investigations, for instance for ore- and oil-seeking [18].

The physical nature of ground conductivity is even today not fully explained, but the most important causes of variation in  $\epsilon$  and  $\sigma$  have been found by experiments. The influence of temperature and humidity was studied by Ratcliffe and White [14] and Smith-Rose [17] in the beginning of the 1930's, and later by Froot and Sharf, in 1954 [24]. The influence of stratification was demonstrated by Grosskopf and Vogt [1] during the last world war.

#### 4.1 Correlation with geology, and variations in effective ground constants.

There seems to be a certain correlation between ground conductivity and geology. Thus most maps and tables of ground constants are arranged in accordance with geological observations. Owing to this a table of expected ground constants in Norway is arranged in table IV, chapter 7.

The different values of  $\sigma$  vary from approximately 5 mho/m for sea water down to  $10^{-4}$  for dry sand and granite rocks. The dielectric constant seems to vary in a similar manner to  $\sigma$  but only between 100 and 2 for frequencies where  $\epsilon$  is of any importance compared with X.

The main reasons why the  $\sigma$  and  $\epsilon$  values vary within areas with approximately uniform ground are:

- a) Increasing moisture content in the soil causes a large increase in both  $\sigma$  and  $\epsilon$ .
- b)  $\sigma$  and  $\epsilon$  seem to vary very little with temperature above  $+5^\circ\text{C}$ , but the values of both drop radically from  $+5$  to  $-1^\circ\text{C}$ , and thermic hysteresis is observed around the freezing point.
- c) The dielectric constant of geological semi-conductors increases appreciably when the frequency decreases below 100 kc/s. Above this frequency, however, only small variations occur in both  $\epsilon$  and  $\sigma$ , but it is possible that  $\sigma$  will increase at frequencies far above 10 Mc/s.
- d) Stratification in the earth has great influence on the effective ground constants.

Radio-geological mapping is only possible because of the large depth of penetration of radio waves compared with the penetration of significant humidity- and temperature variations. At frequencies above 10 Mc/s seasonal variations may be of importance, and above 100 Mc/s even diurnal variations may be so large that such mapping is without any value because the depth of penetration in wet soil is so small.

## 5.0 MEASUREMENTS IN SOUTHERN NORWAY

The field measurements were carried out on expeditions for 3 to 4 weeks each to different parts of Southern Norway. A survey of these expeditions is presented in Table I and a map is given in Fig. (5.1). Before each departure districts of special interest were selected on detailed geological maps from Norges Geologiske Undersøkelse (NGU), and upon the arrival in these districts, suitable measuring sites were found by inspection. The transmitter was erected where electric power was available, and the measuring equipment was carried to a number of different sites in the vicinity.

Measurements were carried out on the frequency 2.5 Mc/s at all sites and 0.218 Mc/s as far as Kløfta broadcasting station could be received. For further stratification studies 8–10 Mc/s were used, especially in districts with sand and gravel deposits.

Since bare rocks are very common in most of Norway, it is convenient to divide the measurements into two groups according to the ground:

- a) Rocky ground,
- b) Clay, sand and gravel.

The first group includes districts with thin layers of soil or gravel upon the rocks. In the lowland these areas are often covered with forests, and the surface is very rough. It is then difficult to find suitable sites for measurements, but special measurements have shown that sparse vegetation does not introduce measurable disturbances in the surface wave. Thick forest of large trees seems to give larger tilt angles and thereby lower effective conductivity.

Table I. *Chronological list of measuring expeditions.*

Date	Districts	Types of ground studied	Remarks
20.3 -31.3	Helgeroa—Tjølling Sandar	Syenite, clay, gravel	A thin layer of snow
15.4 -29.4	Asker, Hurum, Jøley Rygge, Mysen, Trøgstad	Limestone, granite, essexite, sand and clay, gneiss	Variable weather no snow
25.5 -10.6	Bamble, Langesund Riser, Fie, Nykirke	Gneiss, limestone, granite, arendalite, rhombporphyry	Partly dry weather
2.8 -11.8	Vang, Romedal, Jømna, Haslemo, Grue, Vormsund, Hauersetser, Jess- heim, Kløfta	Clays, sand and gravel and some gneiss	Very dry except the last days
27.9 -3.10	Gudbrandsdal, Trondheim	Sandstone, gravel, clay	Cool and wet weather

The second group consists of areas with thick layers of clay, sand or gravel, and some peat and heath is included. In these districts ideal measuring sites are found without difficulty.

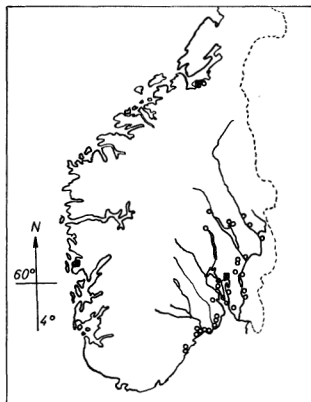


Fig. 5.1. A survey of measuring sites in the Southern Norway.

### 5.1 Investigations in rocky terrain.

Within the rocky terrain measurements were made, as far as possible, on plane, even sites with little or no vegetation. Some examples are shown in Fig. (5.2). The  $\sigma$  and  $\epsilon$  values measured are plotted in Fig. (5.3) and (5.4) respectively.

The selection of sites may appear somewhat fortuitous. This is because a complete mapping was found to be impossible within one year, so an effort was made to correct the German maps [31] only.

The large scattering which appears even within areas of the same type, is supposed first of all to have been introduced by the different water content in the upper layers partly because of changes in the state of disintegration. The granites appear most homogeneous, with a very low conductivity and low dielectric constant. The arendalite at the south coast, however, seems to be better conducting, similar to the gneisses of the Bamble Formation. The gneisses could not be classified because the measurements are too few. The large scattering in  $\sigma$  may partly be due to the fact that no attempt was made to distinguish between the different kinds of gneisses.

The variations in  $\epsilon$  are to some extent correlated to the variations in  $\sigma$ , but at some places very large values were derived. This may verify the assumption of stratification caused by differing moisture content in the upper layer even in rocky ground.

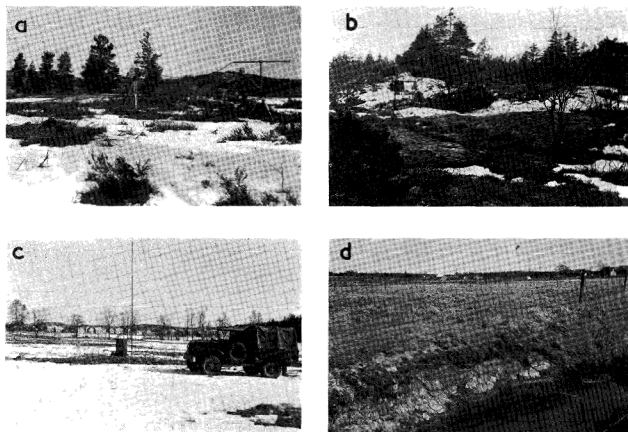


Fig. 5.2. Some examples of measurements in different terrain.

- a) Asker, granite rocks. b) Helgeroa, Vestfold, syenitic rocks. c) Sandar, Truck and transmitter at Raet  
d) Rygge, typical clay area.

### 5.2 Clay, sand and gravel.

The  $\sigma$  and  $\epsilon$  values measured in areas with clay, sand and gravel are plotted in Fig. (5.3) and (5.4) respectively. From these the following conclusions may be drawn:

- These areas are classified as «fairly good» on the German maps, but it appears from the measured values that appreciable differences exist, and that gravel of all kinds is very poor conducting compared with clay.
- Clay in formerly submarine areas, which covers large parts of the Southern Norway, is far better conducting than any rocks. Its dielectric constant is high.

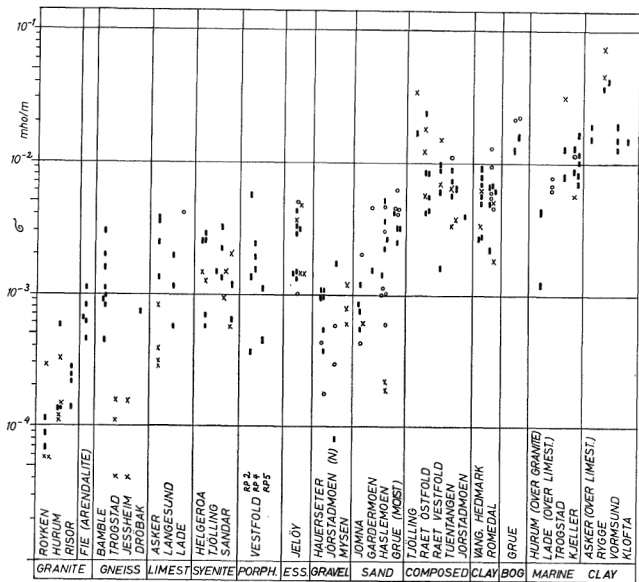
Inland there is clay in glacier and river deposits too. Measurements in Hedmark indicate that these are not as good conducting as those in part b). A similar difference in the conductivity of sand and gravel above and below the «marine limit» is not pointed out.

The difference in the conductivity of sand compared with clay is to some extent counteracted in the lowland sand areas by a sublayer of clay, as for instance along «Raet» through Østfold and Vestfold. Within these areas a number of interesting cases of extreme stratification could be observed.

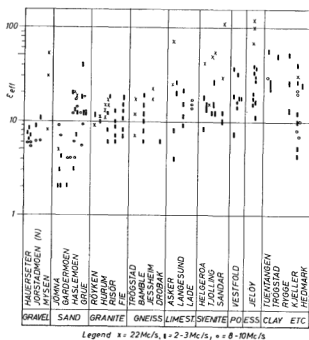
It is worth while noting that marine clays will dominate a site whether it lies as a subsoil under meters of sand or gravel or as a thin layer upon poor conducting rocks. This is easily explained by the great difference in penetration of radio waves into the different media. Three illustrating examples are shown in Fig. (5.5) and Table II.

Sand or gravel in glacier and river deposits which commonly occurs in Norwegian valleys and which is typical at our country drill grounds, shows extremely low values of  $\sigma$  and  $\epsilon$ .

The measurements at Grue where higher values were derived, were carried out on the wet banks of the river Glomma, shown in Fig. (5.5).



Legend: x = .22Mc/s, 1 = 2-3Mc/s, o = 8-10Mc/s



Legend x = 22Mc/s, 1 = 2-3Mc/s, o = 8-10Mc/s

Fig. 5.3. Plots of effective conductivity measured within fairly uniform areas of different ground.

On large wet bogs near Grue very high conductivity was measured together with an effective dielectric constant near 100 at 2.5 Mc/s and about 35 at 8 Mc/s.

### 5.3 Conclusion.

During the wave-tilt measurements in 1955 large variations in both  $\sigma$  and  $\epsilon$  were found within rocky terrain as well as in clay and gravel districts. The local variations are supposed to be due to

Fig. 5.4. Plots of effective dielectric constant measured within fairly uniform areas of different ground.



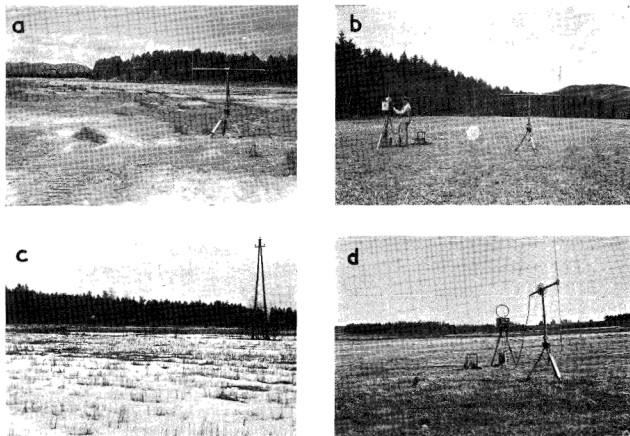


Fig. 5.5. Photographs from the measurements at Grue, Hurum, Tjølling and Rygge.

- a) Grue: On the wet banks of Glomma, fine sand. b) Hurum: A 100 m wide clay zone between granite rocks. c) Tjølling: A clay layer covered with sand between rocks of larvikite-syenite. d) Rygge: In the outskirts of Raet, about 1 m of sand and gravel upon marine clay. Gneissic rocks visible 300 m apart.

Table II. Some measurements made on the sites shown in Fig. (5.5), see also Fig. (5.3) and Fig. (5.4) for comparison.

Fig. 5.5	$f$ Mc/s	$\rho$	$\varphi$ deg.	$\epsilon_{eff}$ appx.	$\sigma_{eff}$ mmho/m	Remarks
a	2.5	0.2	31	12	3	A moderate conductivity even in very wet sand.
b	2.5	0.15	26	27	4.9	The poorly conducting granite gives high $\epsilon_{eff}$ but low $\sigma_{eff}$ at the lowest frequency only
	0.218	0.06	15	240	1.7	
c	2.5	0.085	55	-47	18	$\sigma_{eff}$ is typical for clay $\epsilon_{eff} < 0$ due to the gravel. The rocks are indicated by very high $\epsilon_{eff}$ , but $\sigma_{eff}$ remains large.
	0.218	0.026	33	610	17	
d	2.5	0.08	47	-11	22	$\epsilon_{eff} < 0$ due to the sand. $\epsilon_{eff} \neq$ due to the rocky subground, $\sigma_{eff}$ remains large.
	0.218	0.03	30	555	12	

different water content in the upper layer of the soil.

In spite of these variations it seems reasonable to believe in a correlation between electrical ground constants and geology. The median values for the rocky districts are in accordance with the

German classification, but with regard to sand, gravel and clay areas this classification is not reasonable.

In Table IV, in the last chapter, a revised classification is shown together with medians of measured ground constants.

## 6.0 SPECIAL INVESTIGATIONS

Some investigations were performed in order to study the effect of ice on fresh water, seasonal variations in  $\sigma$  and  $\varepsilon$  in a clay area and the possibility of directional attenuation of surface waves over anisotropic ground at Bamble.

Investigations of this kind ordinarily require a more accurate measuring equipment and much more time, but as the result, qualitatively, was found to be in good agreement with the theory outlined before, some details will be presented.

## 6.1 Stratification studies.

An ice covered lake was expected to yield an idealized case of horizontal stratification, thus testing of the measuring equipment as well as the theory could be carried out. In addition the result would give useful information about the effect of snow and ice in the ground.

Smith-Rose [17] has shown before that 4'' of ice could not be detected by wave tilt measurements at frequencies below 10 Mc/s, so a lake with

very thick ice and deep water was searched out. The northern part of Randsfjorden was found to fulfil both requirements, and measurements were performed near Odnes on March 1 to 3, 1955. The air temperature varied between  $-10$  and  $-5^{\circ}$  C.

The transmitter was erected on the shore, and the measuring equipment situated 900 m apart at two different sites in the middle of the lake:

- On 0.46 m ice + 0.1 m snow upon 40 m of water,
- On a 10 m wide cleared road straight out from the transmitter, on 0.8 m ice and 30 m of water.

Kløfta broadcasting station was received and used for measurements on 0,218 Mc/s, though this transmitter was situated in the opposite direction to our own.

The resulting  $\varrho$  and  $\varphi$  values are plotted in Fig. (6.1).  $\varphi$  is calculated from  $K/\varrho$  as shown in chapter 3.2. The centre of each circle is chosen from the best of three measurements according to the control  $\theta'$ , but all three measurements are covered by

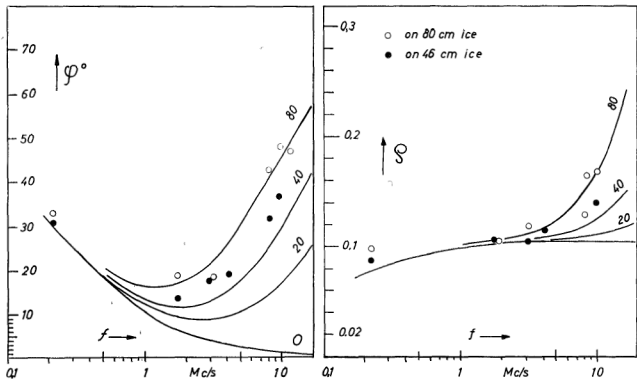
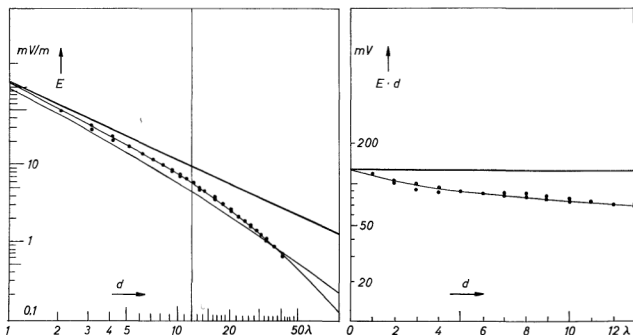


Fig. 6.1. Measurements of wave tilt on an ice covered lake. (Randsfjord 1955).

Fig. 6.2. Field strength measurements on Randsfjord,  $f = 11.1$  Mc/s.

the circle. The «0» curve is calculated for homogeneous ground with  $\epsilon_2 = 90$  and  $\sigma_2 = 1.8$  mmho/m. This is a little higher than expected for fresh water, but these values suit best in the low frequency range.

It is obvious that the ice introduces appreciable changes in both  $\rho$  and  $\varphi$  at frequencies above 2 Mc/s. For further comparison with the theory three additional curves are drawn in accordance with equation (2.21) for a surface layer with  $\epsilon_1 = 4$ ,  $X_1 \ll \epsilon_1$  and the thickness  $Z = 20, 40$  and  $80$  cm respectively [20].

It is seen that the ice thickness at point a) does not fit perfectly, this may be due to faulty measurement of the ice or because the snow was neglected, anyhow the variation in  $\rho$  and  $\varphi$  with increasing frequency is convincing.

Just after the wave tilt measurements a field strength profile was measured in a straight line from the transmitter through point a) on the frequency 11.1 Mc/s. A very high accuracy was obtained by keeping the receiver continually running while it was transported on a toboggan. All the measurements were repeated on the return. The field strength values are plotted in Fig. (6.2). The curve through the plots in Fig. (6.2) is calculated by means of Norton's field strength curves [7] where the numerical distance  $p, b$  is derived

from equation (2.06) after extrapolation of a curve through the measured  $\rho$  and  $\varphi$  values plotted in Fig. (6.1). The intersecting curve yields fresh water only.

The connection between wave-tilt and field strength attenuation is in good agreement with the theory. For further investigation of Wait's attenuation curves for extreme stratification, higher frequencies should be employed.

For evaluation of the  $\rho$  and  $\varphi$  curves, see the Appendix.

It is almost a paradox that the pronounced increase in  $\varphi'$  through the short wave region, though entirely due to the poor conductivity of the upper layer, causes a remarkable increase in the effective ground conductivity. At short distance from the transmitter this leads to a reduced attenuation of the surface waves, but since  $\rho'$  also increases, the long range attenuation will increase.

## 6.2 Seasonal variations.

As mentioned in chapter 4.2, both  $\sigma$  and  $\epsilon$  are subject to changes with variation in the moisture content and temperature of the soil. The effective ground constants, however, are expected to remain fairly constant.

In order to study the actual changes in effective ground constants during periods of extremely

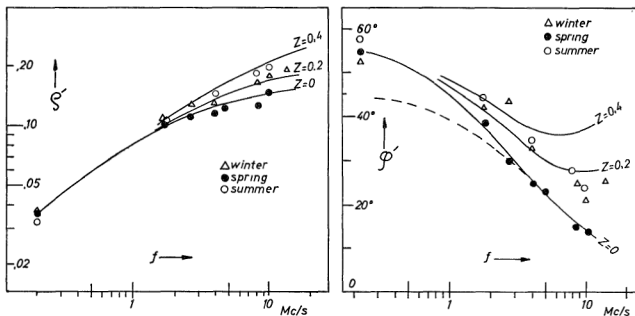


Fig. 6.3. Seasonal variations in wave tilt observed at Kjeller airport 1955.

different weather, 3 series of measurements were performed at Kjeller airport in 1955:

- February 22—23, dry air, 1 foot of snow, ground frozen, air temperature  $-5$  to  $-10^{\circ}$  C in the day,  $-30^{\circ}$  C at night for more than one week before the measurements.
- May 13—16, no snow or ice, very wet ground after heavy rain,  $+10^{\circ}$  C.
- July 26—28, dry air, very dry earth surface after weeks without raining, shade temperature  $+30^{\circ}$  C.

The measurements were carried out at frequencies between 10 and 1.75 Mc/s, and additional

measurements were performed on the frequency of Kløfta, 0.218 Mc/s.

The terrain was ideal for wave tilt measurements, being a flat clay area covered with short grass only and ordinarily with a very wet ground. The results of the measurements are presented in Fig. (6.3) showing  $q'$  and  $\varphi'$ , the latter being calculated from  $K|q'$ .

From the usual analysis the effective ground constants plotted in Fig. (6.4) are derived.  $\sigma_{eff}$  is clearly almost independent of weather changes as well as of frequency variations.  $\epsilon_{eff}$  on the other hand is negative for frequencies below 2 Mc/s in all cases, fairly constant for frequencies above 4 mc/s, but does indeed vary according to weather changes.

The effect of the corresponding variations in surface wave attenuation is demonstrated in Fig. (6.6).

The variations may to a large extent be explained by means of the stratification theory. For this purpose we introduce a simplified model and assume an infinitely deep sub-ground of high conductivity (2) upon which an upper layer (1) is formed by frost in the winter and drought in the summer. For further simplification we assume the ground to be homogeneous in the spring b) with  $\sigma = \sigma_2 = 13$  mmho/m and  $\epsilon_r = \epsilon_2 = 50$ . This gives the  $\epsilon_0$  curves in Fig. (6.5) calculated by equation (2.04).

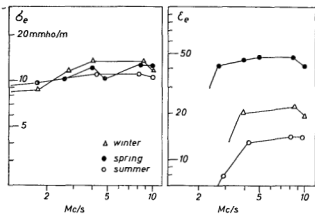


Fig. 6.4. Effective ground constants according to Fig. 6.3 (Kjeller 1955).

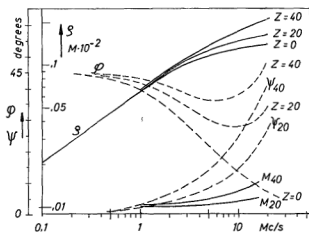


Fig. 6.5. Frequency variations in  $\theta$ ,  $\varphi$  and  $M$ ,  $\psi$  for a good conducting subground covered with a poor conducting surface layer.

If a surface layer exists upon this sub-ground, with the thickness  $Z$ ,  $\sigma_1 = \sigma_0/10$  and  $\epsilon_1 = \epsilon_0/10$ , we obtain from chapter 2.2 a correction factor

$$|M| e^{i\psi} = \tanh(\alpha + u_1 Z) \quad (2.18)$$

where

$$\delta \approx \frac{\sqrt{\epsilon'_1 - 1}}{\epsilon'_1} \frac{\epsilon'_2}{\sqrt{\epsilon'_2 - 1}} \approx \frac{1}{0.340} \quad (2.22)$$

gives  $\alpha = \tanh^{-1} 0.34 \approx 0.345$ , and from equation (2.08):

$$u_1 Z = \sqrt{h^2 + \gamma_1^2} Z \approx j\gamma_0 \sqrt{\epsilon'_1 - 1} Z \\ \approx j 2.09 \cdot 10^{-2} f_{(Mc/s)} \sqrt{\epsilon'_1 - 1} Z_{(m)} \quad (6.01)$$

Consequently  $(\alpha + u_1 Z)$  may be calculated for different  $f$  and  $Z$ , and the correction factor is found. The wave tilt is then easily derived from:

$$\theta' e^{i\psi'} \approx |M| |Q_2 e^{i(\varphi_2 + \psi)}| \quad (2.21)$$

The last expression is plotted against frequency in Fig. (6.5) together with magnitude and phase of the correction factor for  $Z = 20$  and 40 cm.

If we now take a look at Fig. (2.3), we find that for  $\theta$  around 0.1 a slight increase in  $\theta$  combined with a large increase in  $\varphi$  will give just the constancy in  $\sigma$  and the large variations in  $\epsilon$  which were shown by the measurements. By further comparison between Fig. (6.5) and Fig. (6.3) it seems obvious that an explanation of the seasonal variations has been found. The most significant discrepancy occurs in the low frequency range where the measurements indicate an additional

boundary surface in the ground, as the  $\varphi$  value for an homogeneous substratum would follow the dotted curve in Fig. (6.3) and never exceed 45 degrees. This has nothing to do with the seasonal variations, however, and the calculated stratification curves are simply superimposed on even curves through the spring measurements to demonstrate the tendency of variation in Fig. (6.3).

Of course this simple model did not explain every detail in the variations, and it is not reasonable to believe that the upper layer is homogeneous in the summer, because the variation in humidity should rather be exponential. It is, however, interesting to note that a reduction in the water content is of far greater importance than an increase in temperature, in as far as the latter alone would give just the opposite result.

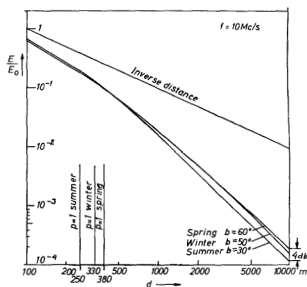


Fig. 6.6. The effect of seasonal variations upon field strength at  $f = 10$  Mc/s (Kjeller).

### 6.3 Directional attenuation at Bamble?

The Bamble formation exhibits a number of different pre-Cambrian rocks, amphibolites, granites, granitic gneisses and several quartzitic rocks, which all form bands from a few millimeters up to several meters wide with a SW-NE strike. Since the dark amphibolites are far better conducting than the light quartzitic rocks, it was expected that the attenuation of surface waves would be greater in a direction perpendicular to the strike than parallel to it.

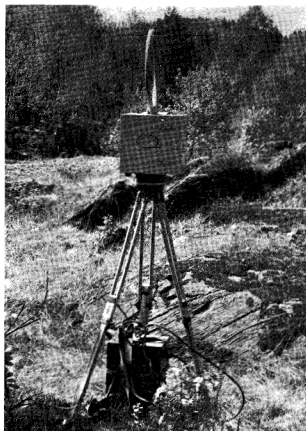


Fig. 6.7. The field strength measuring equipment in an area of banded gneiss at Feset (point 1300mNE).

One week was spent on investigations of the Bamble formation during the summer 1955. On the first three days wave tilt measurements were performed at Riis, and the last days were spent on field strength measurements around Feset.

At Riis 3 sites were chosen for wave tilt measurements, (a, b, c), which were carried out on 2.5 Mc/s twice at each site, with the plane of incidence of the waves parallel to the strike of the rocks and perpendicular to it, respectively ( $\parallel$ ,  $\perp$ ).

The result is shown in Table III. It will be noted that no difference in effective ground constants for waves travelling in the different directions could be seen.

Table III. Ground constants measured at Riis, Bamble.  $f = 2.5$  Mc/s.

Site	$\epsilon_{eff}$		$\sigma_{eff}$ mmho/m	
	$\parallel$	$\perp$	$\parallel$	$\perp$
a	18	32	1,7	3,1
b	19	19	0,83	0,95
c	22	19	1,1	0,97

For the field strength measurements the transmitter was erected in a small meadow near Feset. The field strength was then measured in 5 different directions, at three sites in each direction, namely 100, 1000 and 2000 m from the transmitter. To avoid local variations it was measured at three points 50 m apart on each site except those at 100 m. The measuring equipment was the same receiver which is used for wave tilt measurements, equipped with a loop aerial, as shown in Fig. (6.7). The measurements are plotted in Fig. (6.8).

It is seen that the scattering is great, but the profiles follow to a large extent the calculated attenuation curves for granite (lowest curve) and banded gneiss (next curve). The latter is calculated from a mean value of the measurements at Riis. Two km from the transmitter no higher field strength was measured in the SW and NE directions than in any other. A 300 m long bog in the SW direction caused appreciably higher field strength at 1000 m. However, nothing similar is found in the NE direction, so it seems unreasonable to believe in a more favourable propagation in this direction because of the better conductivity in the rocks. For comparison a curve is drawn to show calculated attenuation along wet bog areas (top curve).

The only conclusion which may be drawn from these investigations is that a directional attenuation of ground waves within the anisotropic areas in the Bamble formation could not be detected by ordinary field measurements. It is supposed therefore that this directional attenuation is of minor

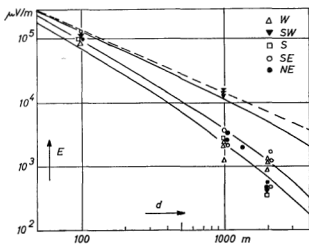


Fig. 6.8. Field strength measurements around Feset, Telemark.  $f = 2,5$  Mc/s.

importance compared with the ordinary ground wave attenuation and the local field disturbances.

It will perhaps be possible to continue the investigations by measuring the complete «radiation

pattern» of a vertical aerial erected at different sites within these districts, but an airplane should be used for the measurements, and it is expected that this will be rather expensive.

## 7.0 THE GROUND CONDUCTIVITY MAP

The purpose of the measurements described was primarily to work out a map of electrical ground constants in Norway. However, no map could be drawn upon the actual measurements only, but by additional study of geological maps, the German military maps and data from measurements in other countries it has been possible to present table IV and the map shown in Fig. (7.1).

The map is to a large extent a reproduction of «Geologisk oversigtskart over Det Sydlige Norge», from 1915. With regard to the rocks a better map was edited in 1953 by Holtedahl and Dons. The old map was chosen because of its presentation of Quaternary deposits and because further details within the gneiss and granite areas could not be utilised. According to small detailed maps from NGU the districts of Quaternary deposits were divided into clay and sand areas. The granite near Oslo was separated from the group of Permian intrusive rocks because of its poor conductivity. Moreover the classification within the Oslo field was simplified by taking account of the electrical similarity of the syenitic, and syendioritic plutonic rocks and the corresponding Permian supra-crustal rocks.

Norwegian geology is extremely complicated, and a correct geological map would require a scale near 1:1. Thus even when the original map was drawn, great simplifications had to be introduced. Neither is Norway fully explored geologically at this moment, so significant clay and sand areas may have escaped our notice. Consequently the map is nothing but a survey, and great care should be taken by using it for classification of small areas. For the latter purpose Table IV is supposed to give more useful information, especially in connection with detailed maps from NGU.

It is obvious both from the measurements at Kjeller and at Randsfjorden that ice in the ground will introduce appreciable changes in the effective ground constants for frequencies above a certain limit, though this effect will be less pronounced in areas with a poor conducting soil. A similar effect is expected to rise when the ground is covered by snow. As far as snows may be regarded a dielectric with relative dielectric constant around 1.5, and, at least for dry snow, a vanishingly small conductivity, the expression for  $M$  in chapter 6.2 shows, however, that no measurable changes in the effective ground constants may be expected at frequencies below 10 Mc/s. Thus the measurements performed on the first expedition, in March, could not be disturbed by the thin layer of snow still remaining on the ground, as shown in Fig. (5.2). But equation (6.01) indicates the possibility of an increase in the ground wave attenuation in the VHF-range during the winter.

### ACKNOWLEDGEMENTS.

The described work was carried out at the Norwegian Defence Research Establishment in close cooperation with the Army Signal Corps. I wish to thank Mr. F. Møller, director of the N.D.R.E., and Mr. F. Lied, chief of research at the Telecommunication dept. N.D.R.E., for allowing me to publish the present work in this form.

I also wish to acknowledge here gratefully the help offered by the staff of Norges Geologiske Undersøkelse, Oslo.

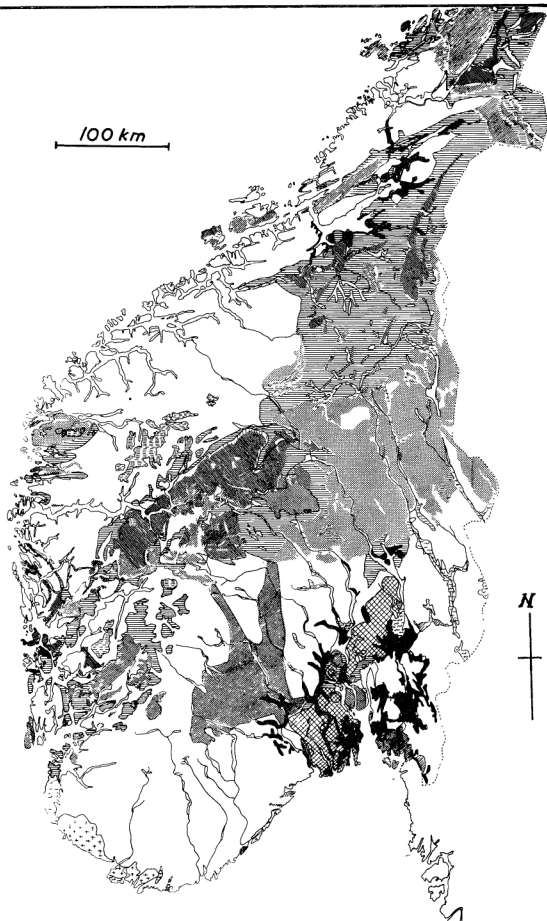












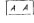






Fig. 7.1. A ground conductivity map of Southern Norway. Symbols are shown in Table IV.



Table IV. *Effective ground constants in Norwegian terrain.*

The relative dielectric constant is presented. The conductivity is given in  $\text{mmho/m} = 10^{-3} \text{ mho/m} = 10^{-14} \text{ emu}$ . The numbers in brackets are very uncertain. Areas with marked stratification are not included. The following classification is employed. E = Extremely-, V = Very-, g = good, p = poor. The classification was originally worked out with a view to propagation of vertically polarized radio waves. Letters in brackets have not been verified by measurements in Norway.

	1		2				3		Symbol Fig. 7.1	
	Assumed values		Measured values				Classification			
	$\epsilon_{eff}$	$\sigma_{eff}$	$f = 0.22$ Mc/s	$\epsilon_{eff}$	$\sigma_{eff}$	$f \geq 2$ Mc/s	$\epsilon_{eff}$	$\sigma_{eff}$		$f < 2$ Mc/s
Sea water .....	81	5000	—	—	—	—	(Eg)	Eg)		
Wet bogs .....	—	—	—	—	30—100	20	Vg	Vg		
Marine clay .....	40	<10	—	10	30—50	15	Vg	Vg		
Fresh water clay....	40	—	—	4	30—50	6	Vg	Vg		
Fresh water .....	80	1—2	—	—	90	1,8	1,8	Vg		
Gabbro .....	20	5	—	—	(20)	—	g	g		
Essexite .....	—	—	(100)	3	25	2	g	g		
Rhombo porphyry ...	10—15	3—5	—	—	15	1,5	g	p		
Syenite (Larvikite) ..	"	"	45	1,2	12	1,5	g	p		
Pulsakite .....	—	—	—	—	—	—	(g	p)		
Cambro—Silurian limestone .....	10—15	3	30	(0,6)	14	1,3	p	p		
Labradorite .....	—	—	—	—	—	—	(p	p)		
Crystalline schist ...	15	3	—	—	—	—	(p	p)		
Sparagmitic sandstone	10	1	—	—	(10)	—	(p	p)		
Gneiss .....	10—15	0,1	15	0,1	12	(1)	Vp	p		
Arendalite .....	—	—	—	—	12	0,8	Vp	p		
Granite .....	6—10	0,1	12	0,12	10	0,15	Vp	p		
Sand .....	5—10	0,1—1	—	—	6—8	2	p	Vp		
Gravel .....	—	—	20	0,6	6—8	0,6	p	Vp		
Ice, glacier .....	3—4	<0,01	—	—	4	—	Ep	Ep		
Snow .....	(1—2)	<<	—	—	—	—	—	(Ep)		

## APPENDIX

Calculation of  $q'$  and  $\varphi'$  for a low-loss ice-layer upon fresh water.

Reference should be made to Fig. (6.1) and Fig. (6.2).

From  $\epsilon'_2 = \epsilon - jX = 90 - j 1.8 \cdot 10^{-3} / \omega \epsilon_0$  the  $\omega_0$  curves are easily derived from equation (2.04), or, since  $\epsilon'_2 \gg 1$ , from:

$$q_2 e^{i\varphi_2} = 1 / \sqrt{\epsilon'_2} \quad (2.11)$$

On taking account of the upper layer (1), the other curves are calculated by means of the correction factor  $M$ . Here  $\epsilon'_1 \approx 4 \cdot j0$  throughout the frequency range in question, and

$$\delta \approx \sqrt{\epsilon'_2 (\epsilon_1 - 1) / \epsilon_1^2} \quad (2.15)$$

yields constant magnitude and vanishing phase angle for frequencies above 1 Mc/s, thus

$$\delta \approx \sqrt{90 \cdot 3 / 16} = 4.11 \text{ and}$$

$$a = \tanh^{-1} (1/4.11) = 0.25$$

In a similar manner the propagation constant  $u_1$  is derived:

$$u_1 \approx j\omega \sqrt{\epsilon_0 \mu_0} \sqrt{\epsilon_1 - 1} \approx j 3.63 \cdot 10^{-8} f \quad (2.08)$$

and the correction factor is calculated from:

$$M = |M| e^{i\psi} = 4.11 \tanh (0.25 + j 3.63 \cdot 10^{-8} f z) \quad (2.18)$$

Now, both magnitude and phase of  $M$  are plotted against frequency allowing  $q'$  and  $\varphi'$  to be derived by graphical superposition according to

$$q' e^{i\varphi'} = |M| [q_2 e^{i(\varphi_2 + \psi)}], \quad (2.21)$$

when a logarithmic scale is employed for  $|M|$  and a linear scale for  $\varphi$  in the graphs.

Note that for higher frequencies the increasing imaginary term of  $(\alpha + u_1 Z)$  will cause oscillatory changes in  $M$ . These variations are analogue to the well known interference phenomena observed by reflection of light from composed dielectric surfaces, demonstrated by Newton's fringes, anti-reflex films etc.

## REFERENCES.

- a) *Fundamental theory.*
- [1] GROSSKOPF, J., and K. VOGT, TFT, 29, 6, 1940, pp. 164—172.
- [2] — HuE, 58, 3, 1941, pp. 52—57.
- [3] GROSSKOPF, J., HuE, 58, 6, 1941, pp. 163—171.
- [4] — HuE, 59, 3, 1942, pp. 71—78.
- [5] — HuE, 60, 5, 1942, pp. 136—141.
- [6] — HFT, 62, 7, 1943, pp.
- [7] NORTON, K. A., Proc. IRE, 29, 12, 1941, pp. 623—639.
- [8] WAIT, J. R., Geophysics, 18, 9, 1953, pp. 416—422.
- [9] — Trans. IRE, Ant./Prop., 1953, pp. 9—11.
- [10] — Geofisica, Milano, 28, 1954, pp. 47—56.
- [11] HAWELKA, R., Vierstellige Tafeln der Kreis- und Hyperbelfunktionen, Braunschweig 1931.
- b) *Measurements etc.*
- See also (1) and (2).
- [12] SMITH-ROSE, R. L., and R. H. BARFIELD, Proc. Royal Soc., A, 1925, pp. 587—601.
- [13] STRUTT, M. J. O., ENT, 7, 10, 1930, pp. 387—393.
- [14] RATCLIFFE, J. A., and F. W. WHITE, Phil. Mag., X, LXV, 1930, pp. 667—680.
- [15] FELDMAN, C. B., Proc. IRE, 21, 1933, pp. 764—800.
- [16] BARFIELD, R. H., Proc. IRE, 75, 1934, pp. 214—220.
- [17] SMITH-ROSE, R. L., Proc. IRE, 75, 1934, pp. 221—235.
- [18] FRITSCH, V., Sml. Vieweg, No. 116, 1939, pp. 1—121.
- [19] HOWE, A. B., BBC Res. Rep., 70, KO62, 1944, pp. 1—5.
- [20] LAMB, J., Trans. Faraday Soc., XLIII, 1946, pp. 238—244.
- [21] GILL, E. W. B., Radio Sec. IEE, 808, 1948, pp. 141—144.
- [22] BRAMSLEV, G., Tekn. Medd. Post og Telegr., Denmark, XVI, 10—11, 1949, pp. 1—14.
- [23] FINE, H., Proc. IRE, 42, 9, 1954, pp. 1405—1408.
- [24] FROOD, D. G. H., and W. A. Sharf, Project Rep. Radio Phys. Lab., Canada, 18-0-8, 1954, pp. 1—75.
- [25] VICE, R. W., Trans. of S. A. Inst. of E. E., April, 1954, pp. 139—150.
- [26] MAZUMDAR, S. C., Journ. of Tel. Eng., New Delhi, 7, 2, 1954, pp. 76—83.
- [27] ELIASSEN, K. E. Graduate work, N.T.H., 1954, not published.
- [28] — NDRE, Int. Rep. T-99, 1954, pp. 1—7.
- [29] — NDRE, Int. Rep. T-103, 1955, pp. 1—16.
- [30] — NDRE, Int. Rep. T-104, 1955, pp. 1—4.
- [31] RICHTER, K., Wehrgeologischer Atlas von Norwegen, Norges Geologiske Undersøkelse, Oslo.
- All geological maps employed are available at Norges Geologiske Undersøkelse, Oslo.
- ENT: Elektrische Nachrichtentechnik,  
HuE: Hochfrequenztechnik und Elektroakustik,  
FTT: Telegraphen- Fernsprech-Funk und Fernsehtechnik.